



The following Communications have been judged by at least two referees to be “very important papers” and will be published online at www.angewandte.org soon:

Z. Zhang, Z. Wang, R. Zhang, K. Ding*

Extremely Efficient Titanium Catalyst for the Enantioselective Cyanation of Aldehydes Using Cooperative Catalysis

Q. Wang, M. Zhang, C. Chen, W. Ma, J. Zhao*

Photocatalytic Aerobic Oxidation of Alcohols on TiO₂: The Acceleration Effect of Brønsted Acids

Y. Fu, Q. Dai, W. Zhang, J. Ren, T. Pan,* C. He*

AlkB Domain of Mammalian ABH8 Catalyzes Hydroxylation of 5-Methoxycarbonylmethyluridine at the Wobble Position of tRNA

H. Braunschweig,* K. Radacki, A. Schneider

Cyclodimerization of an Oxoboryl Complex induced by *trans*-Ligand Abstraction

C. Apostolidis, B. Schimmelpfennig, N. Magnani, P. Lindqvist-Reis,* O. Walter, R. Sykora, A. Morgenstern, E. Colineau, R. Caciuffo, R. Klenze, R. G. Haire, J. Rebizant, F. Bruchertseifer, T. Fanghanel
[An(H₂O)₉](CF₃SO₃)₃ (An=U–Cm, Cf): Exploring Their Stability, Structural Chemistry, and Magnetic Behavior by Experiment and Theory

S. Rizzato, J. Bergès, S. A. Mason, A. Albinati, J. Kozelka*

Dispersion-Driven Hydrogen Bonding: Theoretically Predicted H–Bond between H₂O and Platinum(II) Identified by Neutron Diffraction

D. R. Dreyer, H. Jia, C. W. Bielawski*

Graphene Oxide: A Convenient Carbocatalyst for Facilitating Oxidation and Hydration Reactions



“When I was eighteen I wanted to play football for Scotland. The greatest scientific advance of the last 50 years is the way biology is becoming a molecular science (chemistry) ...”

This and more about David O'Hagan can be found on page 5604.

Author Profile

David O'Hagan _____ 5604

Fluorinated Heterocyclic Compounds

Viacheslav A. Petrov

Books

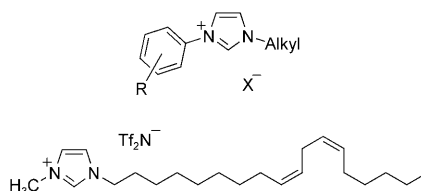
reviewed by G. Weaver _____ 5605

Victor Y.-S. Lin (1966–2010)

Obituary

W. Lin _____ 5606–5607

Melting without heat: Attempts to design new ionic liquids (often functionalized) often lead to only “ionic solids”. Two recent studies demonstrate very promising and viable ways to “liquify” systems that are based on the common structural motifs that still dominate the literature (see picture; Tf₂N[−] = bis(trifluoromethylsulfonyl)imide).



Highlights

Ionic Liquids

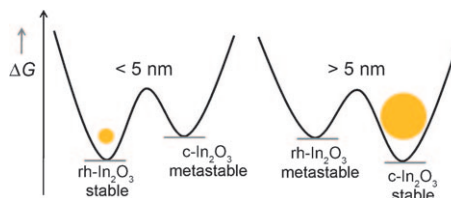
R. Giernoth* _____ 5608–5609

Ionic Liquids with a Twist: New Routes to Liquid Salts

Nanomaterials

A. Gurlo* _____ 5610–5612

Structural Stability of High-Pressure Polymorphs in In_2O_3 Nanocrystals: Evidence of Stress-Induced Transition?



Size matters: Both high-pressure and nanoscale syntheses can lead to the same indium oxide polymorph. Recent work by Farvid et al. provide an explanation: metastable high-pressure rh- In_2O_3 is sta-

bilized by surface forces in nanoscale particles, whereas in larger particles only the stable cubic c- In_2O_3 polymorph exists; this is evident in the energy diagrams.

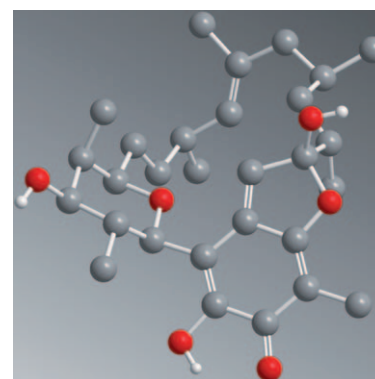
Minireviews

Natural Product Synthesis

H. J. Martin,* T. Magauer,
J. Mulzer* _____ 5614–5626

In Pursuit of a Competitive Target: Total Synthesis of the Antibiotic Kendomycin

The ‘ansa’ my friend: Kendomycin (see structure; O red, C gray) is a carbacyclic ansa compound having unusual structural features and extremely diverse biological activity. This Minireview provides a chronological and comprehensive portrayal of the synthetic work on the synthesis of the title compound from eight research groups. Thus far, five total syntheses and a number of fragment syntheses have been reported.

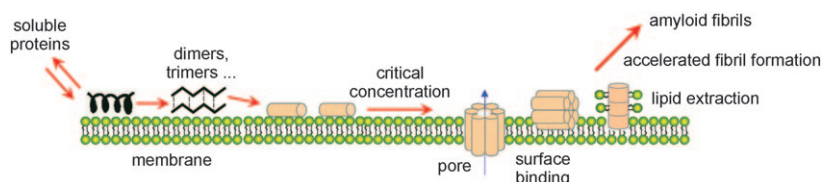


Reviews

Amyloid Toxicity

S. M. Butterfield,
H. A. Lashuel* _____ 5628–5654

Amyloidogenic Protein–Membrane Interactions: Mechanistic Insight from Model Systems



Mutual disruption: Model systems have been used to investigate the mechanisms by which membrane surfaces influence the folding, oligomerization, and fibril formation of amyloidogenic proteins, and

by which these oligomeric protein structures in turn disrupt membrane structural integrity (see picture). These studies have uncovered a number of key mechanistic features that contribute to cytotoxicity.

For the USA and Canada: ANGEWANDTE CHEMIE International Edition (ISSN 1433-7851) is published weekly by Wiley-VCH, PO Box 191161, 69451 Weinheim, Germany. Air freight and mailing in the USA by Publications Expediting Inc., 200 Meacham Ave., Elmont, NY 11003. Periodicals

postage paid at Jamaica, NY 11431. US POSTMASTER: send address changes to *Angewandte Chemie*, Journal Customer Services, John Wiley & Sons Inc., 350 Main St., Malden, MA 02148-5020. Annual subscription price for institutions: US\$ 9442/8583 (valid for print and electronic / print or electronic delivery); for

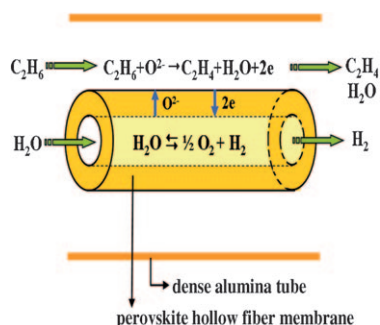
individuals who are personal members of a national chemical society prices are available on request. Postage and handling charges included. All prices are subject to local VAT/sales tax.

Communications

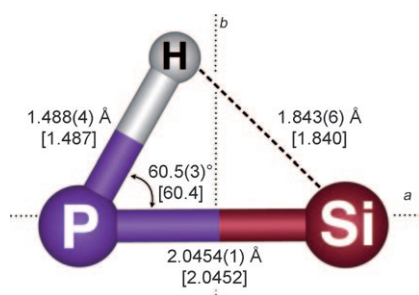
Water Splitting

H. Jiang,* Z. Cao, S. Schirrmeister,
T. Schiestel, J. Caro* — 5656 – 5660

A Coupling Strategy to Produce Hydrogen
and Ethylene in a Membrane Reactor



Burns at both ends: By coupling water splitting and ethane dehydrogenation in a perovskite (BCFZ; $\text{BaCo}_x\text{Fe}_y\text{Zr}_{1-x-y}\text{O}_{3-\delta}$) oxygen-permeable membrane reactor, hydrogen from water splitting was obtained on one side of the membrane, and ethylene was produced simultaneously on the other.

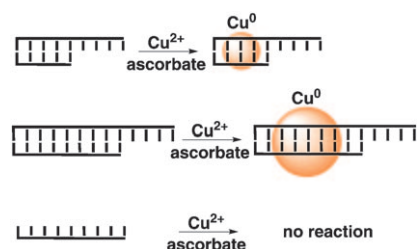


Curiouser and curiouser: By combining high-resolution molecular spectroscopy in the centimeter and millimeter wave regions, and high-level coupled-cluster quantum-chemical calculations, the structure of the HPSi molecule has been determined. The bridged geometry of HPSi is in remarkable contrast to that of the C and/or N analogues, such as HCN/HNC, HCP, and HNSi, which are all linear.

“Heavy” Hydrogen Cyanide

V. Lattanzi, S. Thorwirth, D. T. Halfen,
L. A. Mück, L. M. Ziurys, P. Thaddeus,
J. Gauss,* M. C. McCarthy* — 5661 – 5664

Bonding in the Heavy Analogue of
Hydrogen Cyanide: The Curious Case of
Bridged HPSi



A helping strand: A method to selectively form copper nanoparticles in solution using double-stranded DNA has been developed. The size of the nanoparticles is controlled by the length of the dsDNA template, and single-stranded DNA did not act as a template (see scheme). Single-stranded overhangs in dsDNA were used to prepare a nanostructure in which two metallized dsDNA segments were linked together by a nonmetallized rigid linker.

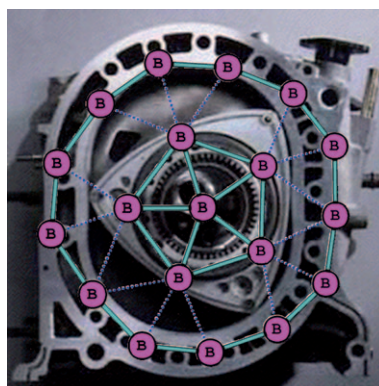
DNA Nanofunctional Units

A. Rotaru, S. Dutta, E. Jentzsch,
K. Gothelf, A. Mokhir* — 5665 – 5667

Selective dsDNA-Templated Formation of
Copper Nanoparticles in Solution



The magic roundabout: The B_{10}^- cluster behaves like a molecular Wankel engine (see picture) in which the two concentric boron rings rotate in opposite directions. During the rotation the cluster remains planar owing to a marginal rotational energy barrier.



Boron Chemistry

J. O. C. Jiménez-Halla, R. Islas, T. Heine,*
G. Merino* — 5668 – 5671

B_{10}^- : An Aromatic Wankel Motor

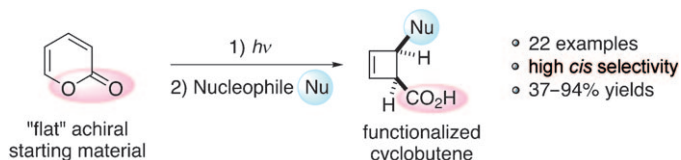


Small-Ring Systems

F. Frébault, M. Luparia, M. T. Oliveira,
R. Goddard, N. Maulide* — **5672–5676**



A Versatile and Stereoselective Synthesis
of Functionalized Cyclobutenes



Square flat: A new atom-economical method for the synthesis of functionalized cyclobutenes has been developed. This versatile sequence hinges upon a unique combination of an elegant photochemical

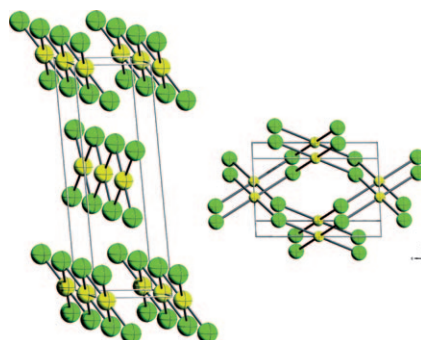
isomerization and a palladium-catalyzed alkylation, and converts the readily available, "flat" aromatic 2-pyrone into a variety of functionalized products with exquisite stereoselectivity.

Polymorphism

J. Evers,* W. Beck, M. Göbel, S. Jakob,
P. Mayer, G. Oehlinger, M. Rotter,
T. M. Klapötke — **5677–5682**



The Structures of δ -PdCl₂ and γ -PdCl₂:
Phases with Negative Thermal Expansion
in One Direction



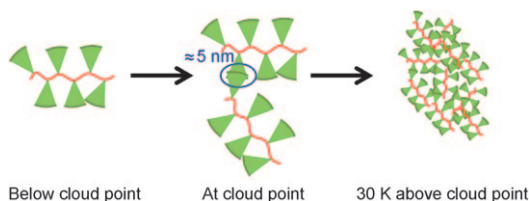
Phase up to reality: In the tetramorphic PdCl₂ system, three of the four phases show a negative thermal expansion in one direction. The two high-temperature phases, α -PdCl₂ and δ -PdCl₂ (see picture; left), contain planar ribbons of edge-connected PdCl₄ squares. The low-temperature phase, γ -PdCl₂ (right), has corrugated layers of corner-connected PdCl₄ squares. It is a link between the ribbon structures (α and δ) and the cluster structure (β) which shows a normal thermal behavior.

Heterogeneous Collapse

M. J. N. Junk, W. Li, A. D. Schlüter,
G. Wegner, H. W. Spiess, A. Zhang,*
D. Hinderberger* — **5683–5687**



EPR Spectroscopic Characterization of
Local Nanoscopic Heterogeneities during
the Thermal Collapse of
Thermoresponsive Dendronized Polymers



The collapse transition of thermoresponsive dendronized polymers was characterized on a molecular scale by CW EPR spectroscopy. Aggregation of the polymer is triggered by dynamic structural

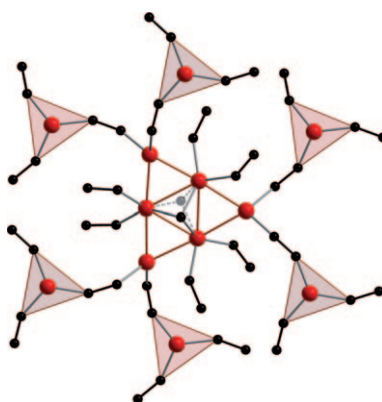
inhomogeneities of a few nanometers, and the dehydration of the polymer chains proceeds, despite the sharp phase transition, over a temperature interval of at least 30 °C (see picture).

Rare Earths Compounds

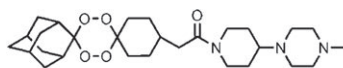
B. Davaasuren, H. Borrmann, E. Dashjav,
G. Kreiner, M. Widom, W. Schnelle,
F. R. Wagner, R. Kniep* — **5688–5692**



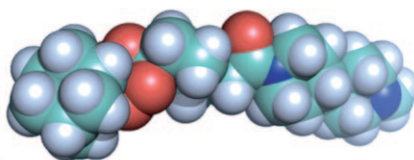
Planar Fe₆ Cluster Units in the Crystal
Structure of RE₁₅Fe₈C₂₅ (RE = Y, Dy, Ho,
Er)



News from Fe–C: The title ternary rare-earth compounds contain planar (magnetic) Fe₆ clusters interlinked by Fe(C₂)₃ units to form polymeric carboferrate complexes (see structure; red Fe, black C). The Fe₆ clusters can be regarded as fragments of γ -Fe and binary iron carbides. The chemical bonding situation in the ternary compounds is characterized by covalent Fe–Fe, polar dative ligand (C₂)→metal (Fe), and Fe→RE interactions.



RKA 182
 $IC_{50} = 0.87 \text{ nM}$
 $ED_{50} = 1.1 \text{ mg kg}^{-1}$
 $ED_{90} = 4.1 \text{ mg kg}^{-1}$
 Solubility $> 40 \text{ mg mL}^{-1} (\text{H}_2\text{O})$



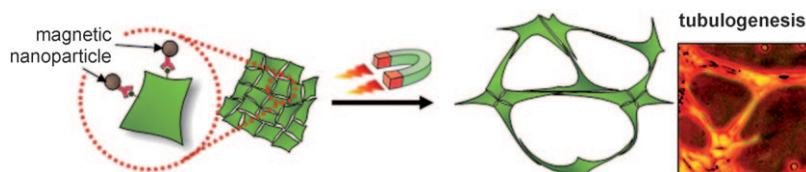
Fighting drug resistance: From a library of over 150 1,2,4,5-tetraoxanes, the candidate RKA 182 was selected for preclinical development as an antimalarial agent. RKA 182 has outstanding in vitro activity

against resistant strains of *P. falciparum* and retains this level of activity against southeast asian isolates that failed artemisinin-based combination therapy.

Antimalarial Agents

P. M. O'Neill,* R. K. Amewu, G. L. Nixon, F. Bousejra ElGarah, M. Mungthin, J. Chadwick, A. E. Shone, L. Vivas, H. Lander, V. Barton, S. Muangnoicharoen, P. G. Bray, J. Davies, B. K. Park, S. Wittlin, R. Brun, M. Preschel, K. Zhang, S. A. Ward — 5693 – 5697

Identification of a 1,2,4,5-Tetraoxane Antimalarial Drug-Development Candidate (RKA 182) with Superior Properties to the Semisynthetic Artemisinins



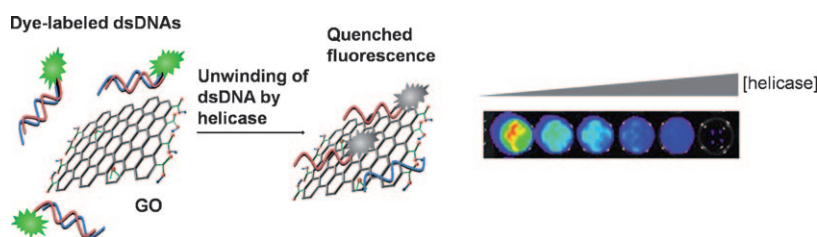
Magnetic attraction: Artificial control of cell activities is achieved by nanoscale magneto-activated cellular signaling (N-MACS), in which magnetic nanoparticles are selectively linked to cell surface receptors and aggregated by an external

magnetic field. Such mechanocellular activation induces downstream cell signaling and initiates tubulogenesis in the preangiogenesis stage of endothelial cells (see picture).

Cellular Signaling

J.-H. Lee, E. S. Kim, M. H. Cho, M. Son, S.-I. Yeon, J.-S. Shin,* J. Cheon* — 5698 – 5702

Artificial Control of Cell Signaling and Growth by Magnetic Nanoparticles



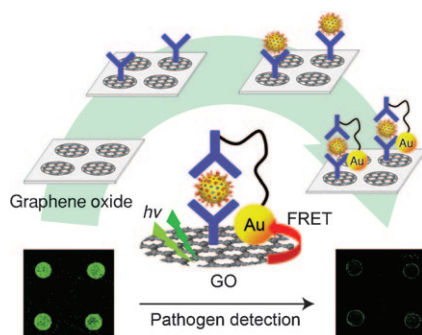
Time to unwind: Graphene oxide (GO) enables the quantitative measurement of helicase-dependent double-stranded DNA (dsDNA) unwinding activity in real time. GO selectively binds to unwound fluo-

rescent-dye-labeled single-stranded DNA and quenches its fluorescence (see picture). The helicase activity is monitored by following the change in fluorescence.

DNA Unwinding

H. Jang, Y.-K. Kim, H.-M. Kwon, W.-S. Yeo, D.-E. Kim, D.-H. Min* — 5703 – 5707

A Graphene-Based Platform for the Assay of Duplex-DNA Unwinding by Helicase



Don't FRET when I GO: Sensitive and selective rotavirus detection is achieved by using the photoluminescence of a graphene oxide (GO) array. The target cell was captured by the rotavirus-specific antibody immobilized on the GO array, and the binding event was monitored by observing the fluorescence quenching that results from fluorescence resonance energy transfer (FRET) between GO and gold nanoparticles linked to the antibodies (see picture).

Biosensors

J. H. Jung, D. S. Cheon, F. Liu, K. B. Lee, T. S. Seo* — 5708 – 5711

A Graphene Oxide Based Immuno-biosensor for Pathogen Detection



Nanorod Synthesis

H. Kim, Y. Chae, D. H. Lee, M. Kim,
J. Huh, Y. Kim, H. Kim, H. J. Kim,
S. O. Kim,* H. Baik, K. Choi, J. S. Kim,
G.-R. Yi, K. Lee* — 5712–5716



Palladium Nanoparticle Catalyzed
Conversion of Iron Nanoparticles into
Diameter- and Length-Controlled Fe₂P
Nanorods



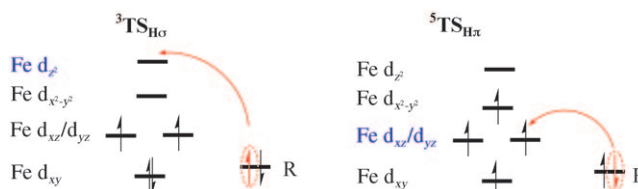
Playing a dual role as a catalyst that destabilizes Fe nanoparticles to form soluble precursors in situ and as a catalytic center for nanorod growth allows Pd nanoparticles to transform Fe nanoparticles and a P source into Fe₂P nanorods (see scheme). The diameter and length of the Fe₂P nanorods can be fine-tuned by means of the diameter of the Pd nanoparticles and the Fe/Pd ratio, respectively.

C–H Bond Activation

C. Geng, S. Ye, F. Neese* — 5717–5720



Analysis of Reaction Channels for Alkane
Hydroxylation by Nonheme Iron(IV)–Oxo
Complexes



New high-spin pathways: All four feasible reaction pathways for alkane hydroxylation by nonheme iron(IV)–oxo complexes have been investigated by computational methods. The triplet σ path is too high in energy to be involved in C–H bond

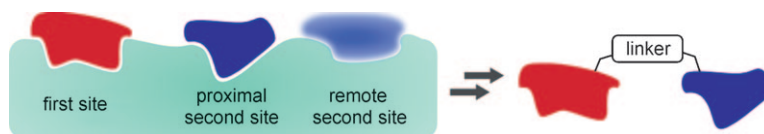
activation, but the reactivity of the quintet π channel competes with the triplet path and may thus offer a new approach for specific control of C–H bond activation by iron(IV)–oxo species (see scheme).

Combinatorial Chemistry

S. V. Shelke, B. Cutting, X. Jiang,
H. Koliwer-Brandl, D. S. Strasser,
O. Schwardt, S. Kelm,
B. Ernst* — 5721–5725



A Fragment-Based In Situ Combinatorial
Approach To Identify High-Affinity
Ligands for Unknown Binding Sites



In the lead: The title method for the identification of ligands is particularly useful for binding sites where little or no structural information is available. In a fragment-based approach, a suitable pair of first- and second-site ligands is identi-

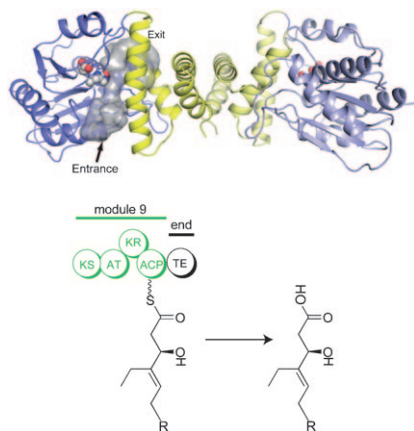
fied by NMR experiments. By applying a receptor-mediated in situ combinatorial approach, the two ligands are then linked to generate a new high-affinity lead structure (see picture).

Natural Products

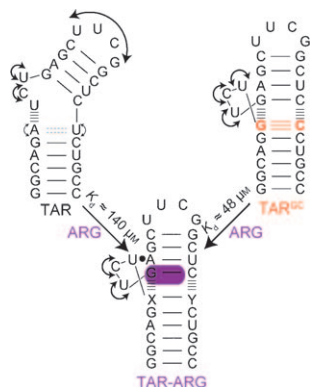
J. B. Scaglione, D. L. Akey, R. Sullivan,
J. D. Kittendorf, C. M. Rath, E.-S. Kim,
J. L. Smith, D. H. Sherman* — 5726–5730



Biochemical and Structural
Characterization of the Tautomycetin
Thioesterase: Analysis of a Stereoselective
Polyketide Hydrolase



A narrow tunnel: Biochemical and structural analysis of the tautomycetin thioesterase (TE) has provided the first high-resolution structure of a linear-chain-terminating TE in polyketide biosynthesis, showing the enzyme to be stereoselective with a constrained substrate chamber relative to macrolactone-forming thioesterases.

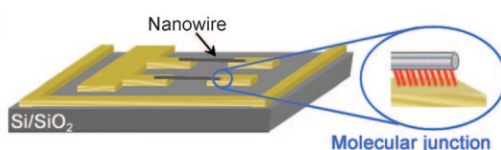
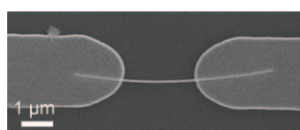


Window of opportunity: Using a single A-U to G-C mutation, the local and global dynamic characteristics of the transactivation response element (TAR) RNA was rationally altered over timescales extending up to milliseconds. This procedure allows it to mimic its bound state with the ligand argininamide (ARG). The mutant binds ARG with slightly enhanced affinity using a conformation indistinguishable from the wild-type sequence.

RNA Dynamics

A. C. Stelzer, J. D. Kratz, Q. Zhang, H. M. Al-Hashimi* 5731–5733

RNA Dynamics by Design: Biasing Ensembles Towards the Ligand-Bound State



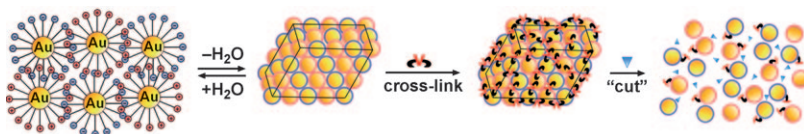
Tunneling to freedom: Plasmons induced by laser irradiation influence the conductivity of a “suspended-wire” molecular junction (see picture). The current enhancement appears to be wavelength- and

laser-power-dependent, and is in semi-quantitative agreement with theoretical models based on a photon-assisted tunneling mechanism.

Plasmons

G. Noy, A. Ophir, Y. Selzer* 5734–5736

Response of Molecular Junctions to Surface Plasmon Polaritons



Seeing is believing: Nanoparticle crystals and core-shell crystals detect and amplify the presence of chemical and enzymatic analytes. These crystals are made insoluble in water by cross-linking their surface

with dithiols incorporating analyte-specific groups. Upon addition of an analyte, these groups are cut, and the “punctured” crystals liberate millions of individual, brightly colored NPs (see picture).

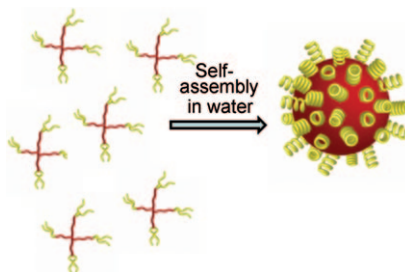
Nanotechnology

B. Kowalczyk, D. A. Walker, S. Soh, B. A. Grzybowski* 5737–5741

Nanoparticle Supracrystals and Layered Supracrystals as Chemical Amplifiers



Special delivery: An effective group A streptococci vaccine is formed from a delivery device consisting of well-defined dendritic structures with nanoscale dimensions (see picture). The structures are designed to display multiple copies of the minimal B-cell epitopes, which were in the optimal conformation on the surface of the nanoparticles. The nanoparticles can be administered without the aid of an adjuvant.



Drug Delivery

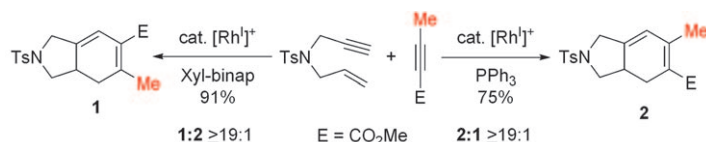
M. Skwarczynski, M. Zaman, C. N. Urbani, I.-C. Lin, Z. Jia, M. R. Batzloff, M. F. Good, M. J. Monteiro,* I. Toth* 5742–5745

Polyacrylate Dendrimer Nanoparticles: A Self-Adjuvanting Vaccine Delivery System



Metal-Catalyzed Reactions

P. A. Evans,* J. R. Sawyer,
P. A. Inglesby _____ **5746–5749**



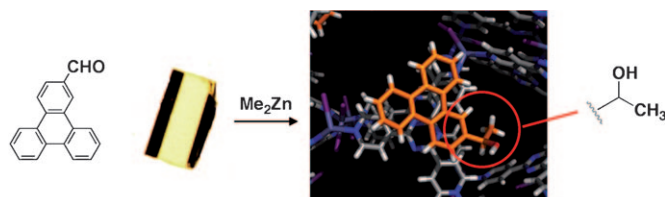
Regiodivergent Ligand-Controlled
Rhodium-Catalyzed [(2+2)+2]
Carbocyclization Reactions with Alkyl
Substituted Methyl Propiolates

Choice is yours: In the title reaction the selective formation of either regioisomer can be controlled through judicious choice of the ancillary ligands (see scheme). Central to this accomplishment

was the realization that residual silver salts from the salt metathesis of the neutral complex have a strong effect on the regio- and diastereoselectivity.

Crystal Engineering

K. Ikemoto, Y. Inokuma,
M. Fujita* _____ **5750–5752**



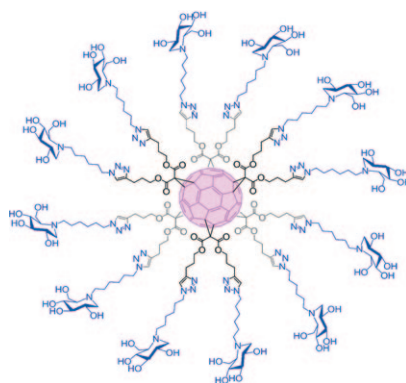
The Reaction of Organozinc Compounds
with an Aldehyde within a Crystalline
Molecular Flask

Organozinc addition reactions were carried out on an aldehyde within a porous coordination network (see picture) in a single-crystal-to-single-crystal fashion, and the product structure was unambiguously

determined by X-ray diffraction. Moreover, a one-pot two-step reaction in a single crystal furnished an ester from an aldehyde without the network losing crystallinity.

Fullerenes

P. Compain,* C. Decroocq, J. Iehl,
M. Holler, D. Hazeldar, T. Mena Barragán,
C. Ortiz Mellet,*
J.-F. Nierengarten* _____ **5753–5756**

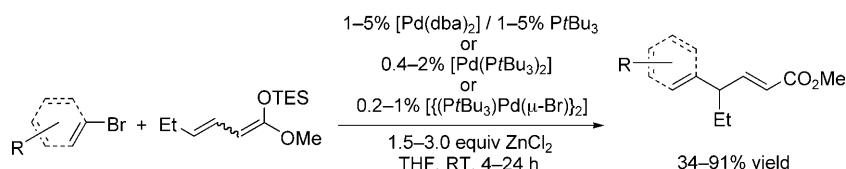


Glycosidase Inhibition with Fullerene
Iminosugar Balls: A Dramatic Multivalent
Effect

Superball! A dodecavalent iminosugar derivative with a fullerene core (see picture) shows a binding enhancement of up to three orders of magnitude over the corresponding monovalent ligand in glycosidase inhibition assays. This is the first evidence of a significant multivalent effect in glycosidase inhibition.

Arylation Reactions

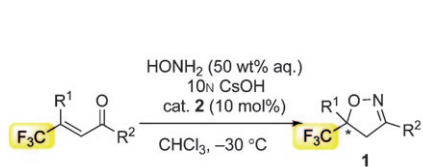
D. S. Huang, J. F. Hartwig* _____ **5757–5761**



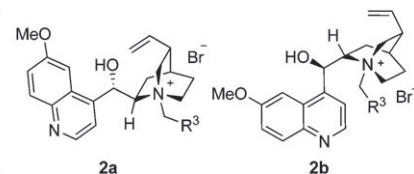
Palladium-Catalyzed γ -Arylation of α,β -
Unsaturated Esters from Silyl Ketene
Acetals

Smarty cat: A method for the palladium-catalyzed γ -arylation of α,β -unsaturated esters via silyl ketene acetals in the absence of fluoride has been developed.

The coupling proceeds with electron-rich and electron-poor aryl bromides and vinyl bromides in high yields with a high tolerance for other functional groups.



Cuts both ways: The title reaction consists of an addition/cyclization/dehydration sequence and affords the biologically important chiral 3,5-diaryl-5-(trifluoromethyl)-2-isoxazolines **1** in excellent yields

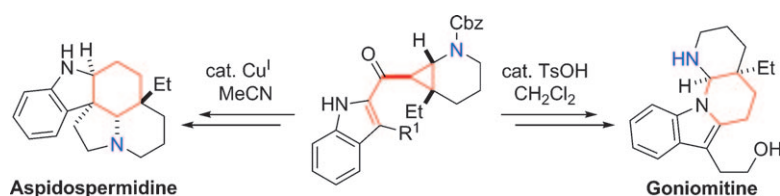


with high *ee* values. The flexibility of accessing either the *S* or *R* enantiomers of the products has been achieved by the appropriate choice of phase-transfer catalyst (**2**).

Organocatalysis

K. Matoba, H. Kawai, T. Furukawa, A. Kusuda, E. Tokunaga, S. Nakamura, M. Shiro, N. Shibata* — 5762 – 5766

Enantioselective Synthesis of Trifluoromethyl-Substituted 2-Isloxazolines: Asymmetric Hydroxylamine/Enone Cascade Reaction



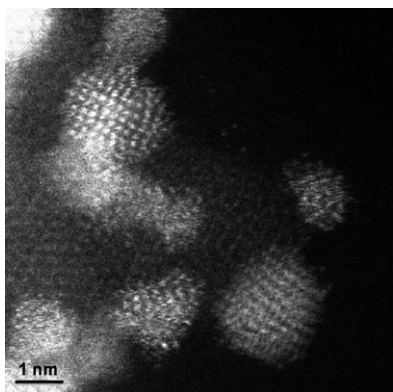
Mild control: Selective cyclization of aminocyclopropanes at either the N1 or C3 position of an indole ring was achieved by tuning the reaction conditions (see scheme). This strategy was applied to the formal synthesis of aspidofermidine and

the total synthesis of goniomitine, which demonstrated significant cytotoxicity against several tumor cell lines (IC_{50} = 150–400 nM). Cbz = benzyl-oxycarbonyl, Ts = 4-toluenesulfonyl.

Alkaloids

F. De Simone, J. Gertsch, J. Waser* — 5767 – 5770

Catalytic Selective Cyclizations of Aminocyclopropanes: Formal Synthesis of Aspidofermidine and Total Synthesis of Goniomitine

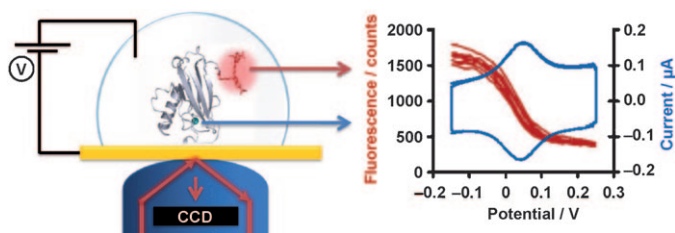


The shape of gold: The title catalyst has been prepared through a colloidal deposition method. Scanning transmission electron microscopy studies confirmed that for the catalyst, gold clusters with a bilayer structure and a diameter of about 0.5 nm are not mandatory to achieve the high activity (see image).

Nanoparticles

Y. Liu, C.-J. Jia, J. Yamasaki, O. Terasaki, F. Schüth* — 5771 – 5775

Highly Active Iron Oxide Supported Gold Catalysts for CO Oxidation: How Small Must the Gold Nanoparticles Be?



Variations in the formal electrochemical potential (E_0) and electron-transfer rates (k_0) of the blue copper protein azurin have been directly observed. A new method, fluorescent cyclic voltammetry (FCV), was used to resolve the properties of 100–

1000 proteins. On this scale, the presence of large variations in the values of both E_0 and k_0 could be established and several forms of heterogeneity were differentiated.

Electrochemistry

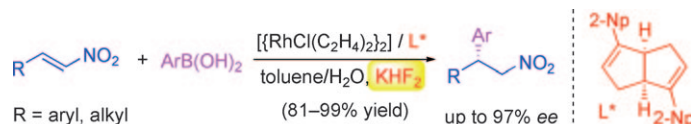
J. M. Salverda, A. V. Patil, G. Mizzon, S. Kuznetsova, G. Zauner, N. Akkiliç, G. W. Canters, J. J. Davis,* H. A. Heering, T. J. Aartsma* — 5776 – 5779

Fluorescent Cyclic Voltammetry of Immobilized Azurin: Direct Observation of Thermodynamic and Kinetic Heterogeneity



Asymmetric Catalysis

Z.-Q. Wang, C.-G. Feng, S.-S. Zhang,
M.-H. Xu,* G.-Q. Lin* **5780–5783**



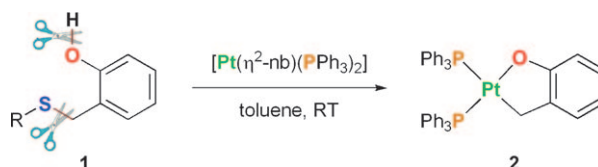
Rhodium-Catalyzed Asymmetric Conjugate Addition of Organoboronic Acids to Nitroalkenes Using Chiral Bicyclo[3.3.0] Diene Ligands

Old before I diene: An efficient rhodium/diene-catalyzed asymmetric conjugate addition of organoboronic acids to challenging nitroalkene substrates that lack

α substituents has been developed. Chiral bicyclo[3.3.0] dienes were found to be superior ligands under $\text{ArB(OH)}_2/\text{KHF}_2$ conditions. Np = naphthyl.

Oxaplatinacycles

N. Nakata, N. Furukawa, T. Toda,
A. Ishii* **5784–5787**



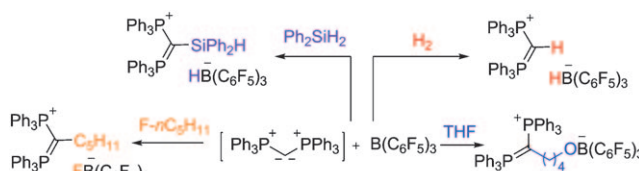
Cleavage of C–S and O–H Bonds by Platinum(0) Complexes To Give Five-Membered 1,2-Oxaplatinacycles

Spectacular platinum(0): 1,2-Oxaplatinacycles **2** were formed unexpectedly from 2-hydroxybenzyl sulfide derivatives **1** by bond cleavage mediated by platinum(0) (see scheme; nb = norbornene). The thermal reaction of **2** gave novel six-

membered 1,2,3-oxaphosphaplatinacycles through ring expansion accompanied by the insertion of a phosphorus atom into the Pt–O bond and the 1,2-shift of a phenyl group.

Frustrated Lewis Pairs

M. Alcarazo,* C. Gomez, S. Holle,
R. Goddard **5788–5791**



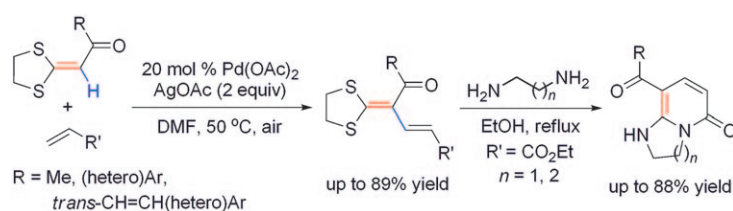
Exploring the Reactivity of Carbon(0)/Borane-Based Frustrated Lewis Pairs

Twice frustrated: The unusual electronic distribution around the central carbon(0) atom in carbodiphosphoranes makes this center so basic that, even after a first

alkylation step, it is still able to act as a cationic Lewis base in the framework of frustrated Lewis pair chemistry.

C–H Bond Activation

H. F. Yu, W. W. Jin, C. L. Sun, J. P. Chen,
W. M. Du, S. B. He,
Z. K. Yu* **5792–5797**



Palladium-Catalyzed Cross-Coupling of Internal Alkenes with Terminal Alkenes to Functionalized 1,3-Butadienes Using C–H Bond Activation: Efficient Synthesis of Bicyclic Pyridones

A highly regioselective direct cross-coupling of internal alkenes of α -oxoketene dithioacetals with terminal alkenes has been successfully realized by palladium-catalyzed C–H bond activation, affording

functionalized 1,3-butadienes. Condensation of the resultant 1,3-butadienes by diamines efficiently produced potentially bioactive bicyclic pyridone derivatives (see scheme).



Supporting information is available on www.angewandte.org (see article for access details).



A video clip is available as Supporting Information on www.angewandte.org (see article for access details).

Sources

Product and Company Directory

You can start the entry for your company in "Sources" in any issue of *Angewandte Chemie*.

If you would like more information, please do not hesitate to contact us.

Wiley-VCH Verlag – Advertising Department

Tel.: 0 62 01 - 60 65 65

Fax: 0 62 01 - 60 65 50

E-Mail: MSchulz@wiley-vch.de

Service

Spotlight on Angewandte's
Sister Journals _____ 5600–5602

Keywords _____ 5798

Authors _____ 5799

Vacancies _____ 5599

Preview _____ 5801

Corrigendum

In a series of papers predating the current frustrated Lewis pair (FLP) terminology, the hydrosilation of carbonyl^[1] and imine^[2] functions as well as the silation of alcohols^[3] has been achieved. Strong kinetic arguments point towards a Si–H bond activation via a FLP-type mechanism in these processes. The authors would like to thank Prof. W. E. Piers for bringing this precedent to their attention.

Exploring the Reactivity of Carbon(0)/
Borane-Based Frustrated Lewis Pairs

M. Alcarazo,* C. Gomez, S. Holle,
R. Goddard _____ 5788–5791

Angew. Chem. Int. Ed. **2010**, 49

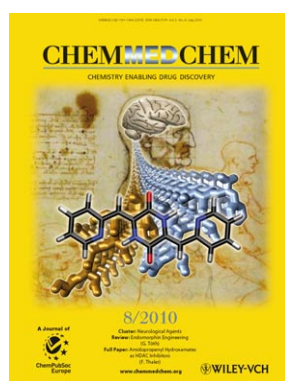
DOI 10.1002/anie.201002119

- [1] a) D. J. Parks, W. E. Piers, *J. Am. Chem. Soc.* **1996**, 118, 9440–9441; b) D. J. Parks, J. M. Blackwell, W. E. Piers, *J. Org. Chem.* **2000**, 65, 3090–3098; c) J. M. Blackwell, D. J. Morrison, W. E. Piers, *Tetrahedron* **2002**, 58, 8247–8254.
[2] J. M. Blackwell, E. Sonmor, T. Scoccitti, W. E. Piers, *Org. Lett.* **2000**, 2, 3921–3923.
[3] J. M. Blackwell, K. L. Foster, V. H. Beck, W. E. Piers, *J. Org. Chem.* **1999**, 64, 4887–4892.

Check out these journals:



www.chemasianj.org



www.chemmedchem.org



www.chemsuschem.org



www.chemcatchem.org